INJECTION OF SUPERNOVA DUST GRAINS INTO PROTOPLANETARY DISKS .

N. Ouellette[1] and **S. J. Desch**[2], [1]Dept. Physics and Astronomy, Arizona State University, PO Box 871504, Tempe AZ 85287 [2]School of Earth and Space Exploration, Arizona State University, PO Box 871404, Tempe AZ 85287 (nicolas.ouellette@asu.edu).

Introduction: Understanding the origins of the short-lived radionuclides (SLR) in the early Solar System is key to understanding the origin and evolution of the Solar System itself. The presence of ^{60}Fe at the time of the formation of the Solar System, with an abundance of $^{60}\mathrm{Fe}/^{56}\mathrm{Fe} \sim 0.3 - 1 \times 10^{-6}$ [1-3] indicates that it was near a massive star that went supernova. No other source can plausibly explain the presence of this radionuclide. Its half-life is too short (1.5 Myr) for it to have been inherited from the interstellar medium [4]. As it is a neutron-heavy isotope, irradiation models produce too little of it [5,6]. Asymptotic-giant-branch stars have been suggested as a source of ^{60}Fe [7,8], but these stars are not commonly found near star-forming regions. The probability of an AGB star contaminating the early solar system is less than 3×10^{-6} [9]. However, massive stars that will explode in a supernova are commonly found in close proxmity to star-forming regions and protoplanetary disks, in regions like the Orion nebula[10], the Carina nebula [11] or NGC 6611 [12] for example. When these massive stars go supernova, the disks, only a few $\times 0.1$ pc from the explosion, will be pelted with SLR-rich ejecta. In this abstract, we review previous results from simulations of the interaction between a protoplanetary disk and gaseous ejecta, and then discuss new results regarding the injection into the disk of SLR-bearing supernova dust grains condensed from the ejecta.

Previous work by Ouellette et al. (2007) [13] has focussed on the interaction between a protoplanetary disk and supernova ejecta hitting it face on. A 2-D hydrodynamics code, based on the Zeus algorithms [14], was written to quantify this interaction. In addition to the features included in Zeus, gas cooling was added to increase the accuracy of the simulation, and a color field was added to follow the position of the gaseous ejecta in the simulation. The adequacy of the numerical resolution used (typically 76 x 120 zones) was demonstrated by using several global quantities to compare to a higher-resolution run (156 x 240 zones). The quantities (e.g., globally mass-weighted velocities and velocity dispersions), identical to those used by [15] to test for numerical convergence, plus quantities unique to our case (mass injected into the disk, mass lost from the disk), agreed to within 10% for the two runs, indicating reasonable convergence. Simulations were made varying a number of parameters including distance from the supernova, the supernova explosion energy and the protoplanetary disk mass. It was found that, in all simulations, a bow shock forms early on, protecting the disk as it deviates the gas around it. The disk easily survives the collision with the gaseous ejecta with very little mass loss ($< 1\%$). It was also found that some of of the gaseous ejecta was mixed in via Kelvin-Helmholtz instabilities; however only a small fraction $\sim 1\%$ of the intercepted ejecta finds its way into the disk.

Most of the gaseous ejecta flows around the disk, with a very small fraction being injected into the disk. If only the gaseous ejecta is considered, this injected amount would be insufficient to explain the SLR ratios seen in meteorites by about two orders of magnitude. However, SLRs in the supernova ejecta will not be in the gas phase, but will have condensed rapidly into dust grains long before they encounter the protoplanetary disk. As the gas phase passes the bow shock, gets deviated and flows around the disk, but the dust grains will decouple from it and continue their trajectories towards the disk. Their trajectories are governed by the gas drag equation

$$F = -\pi a^2 \, C_{\mathrm{D}} \, \rho_{\mathrm{g}} \, d |\boldsymbol{v}_{\mathrm{d}} - \boldsymbol{v}_{\mathrm{g}}| \, (\boldsymbol{v}_{\mathrm{d}} - \boldsymbol{v}_{\mathrm{g}}), \qquad (1)$$

where a is the radius of the dust, $\boldsymbol{v}_{\mathrm{d}}$ and $\boldsymbol{v}_{\mathrm{g}}$ are the velocities of a dust grain and the gas in its vicinity, and ρ_{g} is the local gas density. The drag coefficient C_{D} is a function of the relative velocities between gas and dust and the gas temperatures, but approaches 2 at highly supersonic relative velocities [16]. As the dust travels towards the disk, drag forces will heat it up, and heat will be radiated away from it, cooling it down. Assuming radiative equilibrium, the dust temperature T_{d} is derived from a balance between frictional drag heating and cooling by emission of infrared radiation:

$$\epsilon\sigma T_{\mathrm{d}}^4 = \epsilon\sigma T_{\mathrm{r}}^4 + \rho_{\mathrm{g}} \, C_{\mathrm{H}} \, (T_{\mathrm{rec}} - T_{\mathrm{d}}) \, , \qquad (2)$$

where σ is the Stefan-Boltzmann constant, and the "recovery temperature" T_{rec} and heating coefficient C_{H} are functions of the gas temperature and the relative velocity between gas and dust [16]. Here a wavelength-averaged emissivity $\epsilon \approx 0.8$ is assumed, and a lower limit to the grain temperature is imposed by including absorption of background radiation with characteristic temperature $T_\mathrm{r} \approx 100$ K. Using these equations, a program was written to follow the trajectories of dust grain using the gas characteristics taken from [13]. A dust grain was positioned at every radial AU, from 4 AU (the innermost boundary) all the way to 40 AU, and followed until it was stopped inside the disk, left the simulation boundary, or burned up by reaching $T_\mathrm{d} = 1500\,\mathrm{K}$. For these simulations, we considered 4 grain diameters: 0.01, 0.1, 1 and 10 microns, consistent with the size distribution of presolar SiC X grains from supernovae [17, 18].

Figure 1 shows the gas isodensity contours and velocity vectors 100 years after the supernova ejecta initially hit the disk, 0.3 pc away. Superimposed on it are the dark lines showing the trajectories of supernova grains with diameters of $0.1\,\mu\mathrm{m}$. These are hardly deflected after passing through the bow shock and are injected with near perfect efficiency into the disk. Larger grains are deflected less, but smaller grains are deflected considerably more, a consequence of their shorter stopping lengths. Figure 2 shows the percentage of dust grains that are injected deep into the disk ($\rho_\mathrm{g} > 10^{-19}\,\mathrm{g\,cm^{-3}}$) as a function of dust diameter. Black denotes the percentage of grains that burn up upon entry. Larger grains ($\sim 10\,\mu\mathrm{m}$) have a greater tendency to evaporate upon entering the disk than grains $0.1 - 1\,\mu\mathrm{m}$ in diameter. Grains smaller than about $0.1\,\mu\mathrm{m}$ tend to be deflected around the disk. The typical diameter of supernova X grains is $0.1 - 1\,\mu\mathrm{m}$ and the mass-averaged injection efficiency is about 30%.

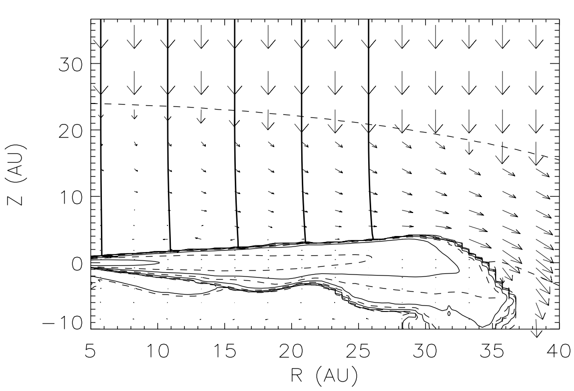

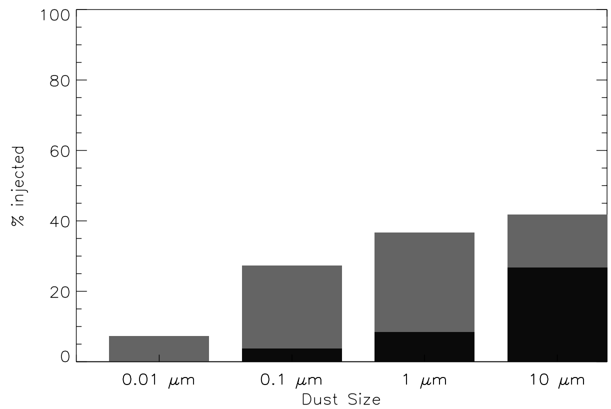

The efficiency of dust injection is insensitive to the distance of the supernova, and should be $\approx$ 30% at a distance of 0.1 pc. If so, then the abundances of SLRs are readily explained. Using the isotopic abundances of supernova ejecta from [19], we calculate initial ratios $^{26}\mathrm{Al}/^{26}\mathrm{Al} = 4.4 \times 10^{-5}$, $^{60}\mathrm{Fe}/^{56}\mathrm{Fe} = 3.7 \times 10^{-7}$, consistent with meteoritic ratios. We are currently conducting a more careful parameter study to better quantify the injection ratios as a function of distance from the supernova. Future calculations will more careful consider the fate of dust as it enters the disk, and investigate mixing of injected radionuclides within the disk.

References:

[1] Tachibana S & Huss G 2003 ApJ 588 41. [2] Huss G & Tachibana S 2004 LPI 35 1811. [3] Mostefaoui S et al. 2004 NewAR 48 155. [4] Harper C 1996 ApJ 466 1026. [5] Lee et al. 1998 ApJ 506 898. [6] Leya et al. 2003 ApJ 594 605. [7] Wasserburg et al. 1994 ApJ 424 412. [8] Cameron et al. 1993, PP III, pp. 47-73. [9] Kastner J & Myers P 1994 ApJ 421 605. [10] McCaughrean M et al. 1996 AJ 111 1977. [11] Smith N et al. 2003 ApJ 587 105. [12] Oliveira J et al. 2005 MNRAS 358 21. [13] Ouellette N et al. 2007 ApJ in revision. [14] Stone J & Norman M 1992 ApJS 80 753. [15] Nakamura F et al. 2006 ApJS 164 477. [16] Gombosi T et al. 1986, Rev. Geophys. 24 667. [17] Hoppe P et al. 2000 MAPS 35 1157. [18] Amari S et al. 1994 GeCoA 58 459. [19] Woosley SE & T Weaver 1995 ApJS 101, 181.